Contribution from the Laboratoire de Chimie de Coordination du CNRS, UP 8241 liée par conventions à l'Université Paul Sabatier et à l'Institut National Polytechnique, 205 route de Narbonne, 31077 Toulouse Cedex, France

New Route to Bimetallic Imidazolate-Bridged Complexes. 6. Structural and Magnetic Consequences of Steric Effects in Mono- and Dinuclear Nickel(II) and Copper(II) Complexes Involving 4-Methylimidazole as Ligand

Jean-Pierre Costes,* Françoise Dahan, and Jean-Pierre Laurent

Received September 18, 1990

The syntheses of (4(5)-methylimidazole)(7-amino-4-methyl-5-aza-3-hepten-2-onato(1−))metal(II)(1+) complexes [metal(II) being nickel(II) and copper(II)] are described. X-ray diffraction and NMR data show that, in both cases, the adjacent isomer (where the methyl group is near the metal ion) is practically missing from the reaction mixture. The remote isomer (methyl group away from the metal ion) of the copper(II) complex crystallizes in the triclinic space group $P\bar{1}$ (No. 2) with two formula weights in a cell having the dimensions a = 9.184 (1) Å, b = 12.828 (2) Å, c = 7.627 (1) Å, α = 94.64 (1)°, β = 105.84 (1)°, and γ = 106.75 (1)°. The related dinuclear complexes (μ-5-methylimidazolato)bis(7-amino-4-methyl-5-aza-3-hepten-2-onato(1−))dimetal(II)(1+) have been obtained. The dinickel complex II_a-4(5)Me crystallizes in the monoclinic space group $P2_1/n$ (No. 14) with four formula weights in the cell having the dimensions a = 15.910 (2) Å, b = 9.769 (1) Å, c = 15.979 (2) Å, and β = 100.31 (2)°. The most interesting result of this structural study is that the coordination plane of one metal ion is nearly orthogonal to the mean plane of the rest of the molecule. Static susceptibility measurements point to an antiferromagnetic exchange interaction of $2J$ = −68 cm^{-1} in the case of the dicopper complex. The mononuclear and dinuclear nickel complexes, which are diamagnetic in the solid state and in noncoordinating solvents, become paramagnetic in the presence of an excess of pyridine. ^1H NMR data seem to indicate that, for the dinickel complex, a modification of the geometry toward coplanarity is needed before adduct formation.

Introduction

In previous papers[1-5] of this series, we have considered several bimetallic (copper and/or nickel) imidazolate-bridged complexes and their mononuclear precursors with the aim of proposing a method to build easily M–Im–M′ units (M and M′ being identical or different metal ions and Im standing for imidazolate ion) with the possibility of varying the nature of M and M′ and the environment of one of them. The synthetic strategy relies on the terdentate ligand AEH (7-amino-4-methyl-5-aza-3-hepten-2-one). In order to fully characterize the mono- and dinuclear complexes, we have investigated their solid-state and solution properties. Preliminary data[2] suggest that methylation of the imidazole (or imidazolate) ring at position 4 may alter the overall geometry of the resulting complexes due to nonbonded interactions of this methyl substituent with the NH_2 or possibly the $OCCH_3$ group of the AEH ligand. From a literature survey,[1,6-15] these interactions are expected either to increase the angle of the M–N(3) and N(3)–C(2) vectors (Figure 1) or to increase the dihedral angle formed by the coordination plane of the metal and the imidazole plane or, in some instances, to favor one isomeric form.

Indeed there are two possible isomers for the mononuclear complexes prepared from 4Me-ImH, depending on the point of attachment of the methyl group to the imidazole ring coordinated to the metal center,[6-8] i.e., the adjacent isomer I_a-4Me (or I_b-4Me) and the remote isomer I_a-5Me (or I_b-5Me). Obviously both situations occur in the dinuclear complexes II_a-4(5)Me (or II_b-4(5)Me), one metal being in an adjacent position with respect to the methyl group and the other metal in a remote position.

In order to decipher the importance and the consequences of this steric demand, we have undertaken a detailed study of copper and nickel complexes deriving from 4-methylimidazole (4Me-ImH). The abbreviations used in the following are quoted in Figure 1.

Table I. Crystallographic Data

(a) $[(AE)Cu(5Me\text{-}ImH)]ClO_4$ (I_b-5Me)	
chem formula $CuClO_5N_4C_{11}H_{19}$	Z = 2
fw = 386.3	$F(000)$ = 398
space group: $P\bar{1}$ (No. 2)	T = 20 ● 1 °C
a = 9.184 (1) Å	λ = 0.71073 Å
b = 12.828 (2) Å	ρ_{obs} = 1.56 g cm^{-3}
c = 7.627 (1) Å	ρ_{calc} = 1.574 g cm^{-3}
α = 94.64 (1)°	μ = 15.3 cm^{-1}
β = 105.84 (1)°	transm coeff = 0.73–1.00
γ = 106.75 (1)°	$R(F_o)$ = 0.034
V = 815.2 (5) Å^3	R_w = 0.038
(b) $[(AE)Ni(4(5)Me\text{-}Im)Ni(AE)]ClO_4$ (II_a-4(5)Me)	
chem formula $Ni_2ClO_6N_6C_{18}H_{31}$	$F(000)$ = 1208
fw = 580.4	T = 20 ± 1 °C
space group: $P2_1/n$ (No. 14)	λ = 0.71073 Å
a = 15.910 (2) Å	ρ_{obs} = 1.56 g cm^{-3}
b = 9.769 (1) Å	ρ_{calc} = 1.578 g cm^{-3}
c = 15.979 (2) Å	μ = 17.0 cm^{-1}
β = 100.31 (2)°	transm coeff = 0.64–1.00
V = 2443 (1) Å^3	$R(F_o)$ = 0.039
Z = 4	R_w = 0.038

Experimental Section

Compounds Preparation. The nickel complexes $[(AE)Ni(5Me\text{-}ImH)]ClO_4$ (I_a-5Me) and $[(AE)Ni(4(5)Me\text{-}Im)Ni(AE)]ClO_4$ (II_a-4(5)Me) were obtained as previously described.[2] Crystals of II_a-4(5)Me were obtained by slow evaporation of a $MeOH/H_2O$ (10/1) solution.

Copper Complexes. $[(AE)Cu(5Me\text{-}ImH)]ClO_4$ (I_b-5Me). A methanolic solution (20 mL) of $Cu(ClO_4)_2 \cdot 6H_2O$ (7 mmol) and of 4Me-ImH (7 mmol) was added with stirring to a BuOH solution (50 mL) of AEH (7 mmol) and triethylamine (7 mmol). The mixture, left overnight, gave crystals of the desired product. They were filtered and dried. Yield: 70%. Anal. Calcd for $C_{11}H_{19}ClCuN_4O_5$: C, 34.2; H, 4.9; N, 14.5; Cu, 16.4. Found: C, 33.9; H, 4.8; N, 14.3; Cu, 16.3.

$[(AE)Cu(4(5)Me\text{-}Im)Cu(AE)]ClO_4$ (II_b-4(5)Me). To 1 mmol of I_b-5Me in 15 mL of MeOH was added with stirring 0.23 mL of a 4.4 M

(1) Costes, J.-P.; Serra, J.-F.; Dahan, F.; Laurent, J.-P. *Inorg. Chem.* **1986**, *25*, 2790.
(2) Costes, J.-P.; Commenges, G.; Laurent, J.-P. *Inorg. Chim. Acta* **1987**, *134*, 237.
(3) Costes, J.-P.; Laurent, J.-P. *Inorg. Chim. Acta* **1987**, *134*, 245.
(4) Costes, J.-P.; Fernandez-Garcia, M.-I. *Inorg. Chim. Acta* **1990**, *173*, 247.
(5) Costes, J.-P.; Laurent, J.-P. *Inorg. Chim. Acta* **1990**, *177*, 277.
(6) Henderson, W. N.; Shepherd, R. E.; Abola, J. *Inorg. Chem.* **1986**, *25*, 3157 and references therein.
(7) Hoq, M. F.; Johnson, C. R.; Paden, S.; Shepherd, R. E. *Inorg. Chem.* **1983**, *22*, 2693.
(8) Shepherd, R. E.; Lomis, T. J.; Koepsel, R. R.; Hedge, R.; Mistry, J. S. *Inorg. Chim. Acta* **1990**, *171*, 139.
(9) Dwyer, P. N.; Madura, P.; Scheidt, W. R. *J. Am. Chem. Soc.* **1974**, *96*, 4815.
(10) Scheidt, W. R. *J. Am. Chem. Soc.* **1974**, *96*, 90.
(11) Storm, C. B.; Freeman, C. M.; Butcher, R. J.; Turner, A. H.; Rowan, N. S.; Johnson, F. O.; Sinn, E. *Inorg. Chem.* **1983**, *22*, 678.
(12) Davis, W. M.; Dewan, J. C.; Lippard, S. J. *Inorg. Chem.* **1981**, *20*, 2928.
(13) McFadden, D. L.; McPhail, A. T.; Garner, C. D.; Mabbs, F. E. *J. Chem. Soc., Dalton Trans.* **1976**, 47.
(14) Bernarducci, E.; Bharadwaj, P. K.; Krogh-Jespersen, K.; Potenza, J. A.; Schugar, H. J. *J. Am. Chem. Soc.* **1983**, *105*, 3860.
(15) O'Young, C. L.; Dewan, J. C.; Lilienthal, H. R.; Lippard, S. J. *J. Am. Chem. Soc.* **1978**, *100*, 7291.
(16) Matsumoto, K.; Ooi, S.; Nakao, Y.; Mori, W.; Nakahara, A. *J. Chem. Soc., Dalton Trans.* **1981**, 2045.

0020-1669/91/1330-1887$02.50/0

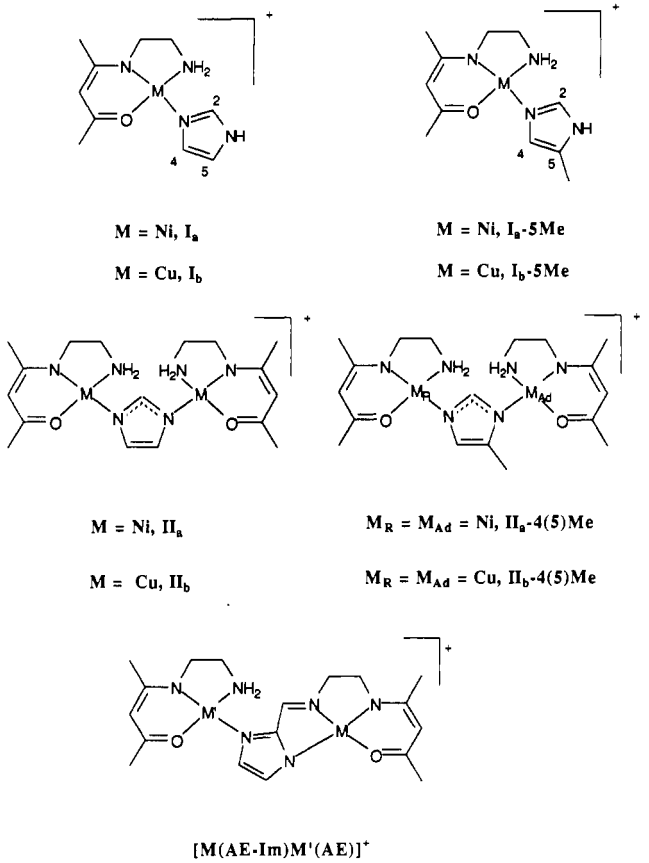

Figure 1. Representation of the mono- and dinuclear complexes considered in the work.

solution of NaOMe. After 1 h, the solution was concentrated under reduced pressure. The resulting precipitate was dissolved in acetone and filtered. The addition of Et_2O to the concentrated solution induced the precipitation of the desired product, which was filtered and dried. Yield: 50%. Anal. Calcd for $C_{18}H_{31}ClCu_2N_6O_6$: C, 36.6; H, 5.3; N, 14.2; Cu, 21.5. Found: C, 36.6; H, 5.2; N, 14.0; Cu, 21.2.

Caution. The compounds reported here were isolated as perchlorate salts. We worked with these compounds in a number of organic solvents without incident, and, as solids, they seem to be reasonably stable to shock and heat. In spite of these observations, the unpredictable behavior of perchlorate salts[17] necessitates extreme caution in their handling.

Physical Measurements. Microanalyses were performed by the Service Central de Microanalyse du CNRS, Lyon, France. Electronic spectra were obtained with a Cary 2390 spectrometer. Magnetic susceptibility data were collected on powdered samples of the compounds with use of a Faraday-type magnetometer using mercury tetrakis(thiocyanato)cobaltate (susceptibility at 20 °C, 16.44×10^{-6} mol^{-1}) as susceptibility standard. Data were corrected for diamagnetism of the ligands and anions (estimated from Pascal constants[18] to be -179×10^{-6} cm^3 mol^{-1} for I_b-5Me and -221×10^{-6} cm^3 mol^{-1} for II_b-4(5)Me and TIP (taken as 60×10^{-6} cm^3 mol^{-1}/Cu atom). ^{1}H NMR spectra were recorded at ambient temperature (295 K) with a Bruker AC 200 spectrometer. All chemical shifts are given in ppm versus TMS with CD_3COCD_3 as solvent. Magnetic susceptibility measurements of complexes in solution were determined by NMR spectroscopy[19] using pyridine as solvent and *tert*-butyl alcohol as indicator.

Crystallography. The experimental details for both complexes are listed in Table I. Crystals were glued on glass fibers and transformed to an Enraf-Nonius CAD4 diffractometer, using graphite-monochromatized Mo Kα radiation.

[(AE)Cu(5Me-ImH)]ClO$_4$ (I_b-5Me). The unit cell was refined by using 25 reflections in the 2θ range 24–30°. A data set of 3205 reflections ($3 < 2\theta < 52°$, $\pm h,\pm k,l$) was recorded as described previously[20] by the $\omega/2\theta$ scan technique (scan width, $0.95° + 0.35° \tan\theta$; scan speed, 1.1–10.1° min^{-1}). The intensities of three standard reflections monitored every 2 h showed no noticeable change. Data reflections monitored were corrected for Lorentz–polarization effects[21] and for empirical absorption corrections.[22] With $F_o^2 > 3\sigma(F_o^2)$, 2712 reflections were considered "observed" and "used" for the structure solution and least-squares refinement.

Table II. Fractional Atomic Coordinates with Esd's in Parentheses for I_b-5Me

atom	x/a	y/b	z/c
Cu	0.30685 (5)	0.73616 (4)	0.78886 (6)
O(1)	0.1494 (3)	0.8078 (2)	0.7706 (4)
C(1)	0.1640 (4)	0.9069 (3)	0.7449 (5)
C(2)	0.2991 (4)	0.9827 (3)	0.7344 (5)
C(3)	0.4483 (4)	0.9647 (3)	0.7548 (5)
C(4)	0.0148 (5)	0.9387 (4)	0.7273 (7)
C(5)	0.5829 (5)	1.0612 (3)	0.7434 (6)
N(1)	0.4686 (3)	0.8700 (2)	0.7830 (4)
C(6)	0.6246 (4)	0.8563 (3)	0.7976 (5)
C(7)	0.6369 (4)	0.7600 (3)	0.8953 (6)
N(2)	0.4835 (3)	0.6688 (3)	0.8272 (5)
N(3)	0.1394 (3)	0.5954 (3)	0.7744 (4)
C(8)	−0.0153 (4)	0.5809 (3)	0.7172 (6)
N(4)	−0.0988 (4)	0.4766 (3)	0.7111 (5)
C(9)	0.0029 (5)	0.4178 (3)	0.7654 (6)
C(10)	0.1497 (5)	0.4930 (3)	0.8035 (6)
C(11)	−0.0525 (6)	0.2976 (4)	0.7685 (8)
Cl	0.4351 (1)	0.35342 (7)	0.6398 (1)
O(2)	0.3291 (4)	0.2521 (3)	0.6537 (5)
O(3)	0.3537 (4)	0.4002 (3)	0.4974 (5)
O(4)	0.5668 (3)	0.3332 (3)	0.5916 (5)
O(5)	0.4954 (4)	0.4288 (3)	0.8104 (4)

The structure was solved by the heavy-atom method using SHELX 76.[23] The atomic scattering factors used were taken from Cromer and Waber[24] for non-hydrogen atoms and from Stewart et al.[25] for hydrogen ones. Completion and refinement of the structure were carried out by different electron density maps and least-squares techniques. All atoms were refined anisotropically, except for the hydrogen atoms, which were observed but introduced in constrained positions (C–H = N–H = 0.97 Å) with an isotropic temperature factor $U = 0.06$ Å^2, kept fixed. The refinement converged with a maximum shift/esd of 0.065 of the final full-matrix least-squares refinement cycle and a maximum peak of 0.3 e/Å^3. The atomic coordinates are listed in Table II.

[(AE)Ni(4(5)Me-Im)Ni(AE)]ClO$_4$ (II_a-4(5)Me). The unit cell was refined by using 25 reflections in the range 22–32°. A data set of 5110 reflections ($3 < 2\theta < 54°$, $\pm h,k,l$) was recorded as I_b-5Me by the $\omega/2\theta$ scan technique (scan width, $1.00° + 0.35° \tan\theta$; scan speed, 1.0–8.2° min^{-1}). The intensities of three standard reflections monitored every 2 h showed a linear decay of about 5% during data collection. Data reflections were corrected for Lorentz–polarization effects and linear decay[21] and for empirical absorption corrections.[22] From the 4944 independant reflections ($hk0$ and $\bar{h}k0$ merged, $R_{av} = 0.0017$), 3079 with $F_o^2 > 3\sigma(F_o^2)$ were retained and used for the structure solution and least-squares refinement.

The structure was solved and refined as I_b-5Me. A slight disorder on perchlorate's oxygen atoms explains their high thermal parameters.

The refinement converged with a maximum shift/esd of 0.060 on the final full-matrix least-squares refinement cycle and a maximum peak of 0.5 e/Å^3. The atomic coordinates are listed in Table III.

Results and Discussion

Our synthetic route yields almost exclusively one type of mononuclear isomer, which, on the basis of structural determination and spectroscopic data, is the remote isomer. In the case of the nickel complex minor amounts of the adjacent isomer I_a-4Me are

(17) Everett, K.; Graf, F. A., Jr. In *CRC Handbook of Laboratory Safety*, 2nd ed.; Steere, N. V., Ed.; Chemical Rubber Co.: Cleveland, OH, 1971.
(18) Pascal, P. *Ann. Chim. Phys.* **1910**, *19*, 5.
(19) Evans, D. F. *Proc. Chem. Soc.* **1958**, 115.
(20) Mosset, A.; Bonnet, J.-J.; Galy, J. *Acta Crystallogr., Sect. B* **1977**, *B33*, 2639.
(21) *SDP Structure determination Package*; B. A. Frenz & Associates, Inc. and Enraf-Nonius: College Station, TX, and Delft, Holland, respectively, 1985.
(22) North, A. C. T.; Phillips, D. C.; Mathews, F. S. *Acta Crystallogr., Sect. A* **1968**, *A24*, 351.
(23) Sheldrick, G. M. *SHELX76. Program for Crystal Structure Determination*; University of Cambridge: Cambridge, England, 1976.
(24) Cromer, D. T.; Waber, J. T. In *International Tables for X-ray Crystallography*; Ibers, J. A., Hamilton, W. C., Eds.; Kynoch Press: Birmingham, England, 1974; Vol. IV, Table 2.2.B, p 99. Cromer, D. T. *Ibid.*; Table 2.3.1, p 149.
(25) Stewart, R. F.; Davidson, E. R.; Simpson, W. T. *J. Chem. Phys.* **1965**, *42*, 3175.

Table III. Fractional Atomic Coordinates with Esd's in Parentheses for II_a-4(5)Me

atom	x/a	y/b	z/c
Ni(1)	0.18591 (3)	0.71561 (6)	0.16862 (4)
O(1)	0.1758 (2)	0.8987 (3)	0.1428 (2)
C(1)	0.1046 (3)	0.9638 (5)	0.1185 (3)
C(2)	0.0261 (3)	0.9139 (5)	0.1237 (3)
C(3)	0.0097 (3)	0.7830 (5)	0.1517 (3)
C(4)	0.1164 (3)	1.1049 (5)	0.0853 (4)
C(5)	−0.0818 (3)	0.7492 (6)	0.1561 (4)
N(1)	0.0709 (2)	0.6919 (4)	0.1732 (2)
C(6)	0.0537 (3)	0.5588 (5)	0.2075 (3)
C(7)	0.1138 (3)	0.4605 (5)	0.1781 (3)
N(2)	0.1985 (2)	0.5254 (4)	0.1963 (3)
N(3)	0.3030 (2)	0.7315 (4)	0.1577 (2)
C(8)	0.3701 (3)	0.6546 (5)	0.1916 (3)
N(4)	0.4432 (2)	0.7003 (4)	0.1731 (2)
C(9)	0.4221 (3)	0.8139 (5)	0.1225 (3)
C(10)	0.3363 (3)	0.8321 (5)	0.1143 (3)
C(11)	0.4852 (3)	0.8949 (6)	0.0881 (4)
Ni(2)	0.55445 (4)	0.62999 (7)	0.21233 (4)
O(2)	0.5615 (2)	0.7388 (4)	0.3074 (2)
C(12)	0.6226 (3)	0.7361 (6)	0.3728 (3)
C(13)	0.6947 (4)	0.6564 (7)	0.3770 (4)
C(14)	0.7145 (3)	0.5727 (7)	0.3149 (4)
C(15)	0.6102 (4)	0.8265 (7)	0.4437 (3)
C(16)	0.8008 (4)	0.5037 (8)	0.3309 (5)
N(5)	0.6617 (3)	0.5507 (5)	0.2420 (3)
C(17)	0.6862 (4)	0.4672 (8)	0.1753 (5)
C(18)	0.6071 (4)	0.4143 (7)	0.1221 (4)
N(6)	0.5452 (3)	0.5255 (5)	0.1104 (3)
Cl	0.1719 (1)	0.7956 (2)	0.4464 (1)
O(3)	0.0983 (5)	0.8458 (10)	0.4580 (5)
O(4)	0.1817 (5)	0.7725 (12)	0.3664 (4)
O(5)	0.2323 (7)	0.8921 (9)	0.4626 (6)
O(6)	0.1895 (6)	0.6906 (10)	0.4966 (7)

Table IV. Selected Bond Lengths (Å) and Angles (deg) with Estimated Standard Deviations in Parentheses for I_b-5Me

Cu–O(1)	1.906 (3)	Cu–N(2)	2.013 (4)
Cu–N(1)	1.933 (3)	Cu–N(3)	1.978 (3)
O(1)–Cu–N(1)	92.8 (1)	N(1)–Cu–N(2)	85.0 (1)
O(1)–Cu–N(2)	175.4 (1)	N(1)–Cu–N(3)	175.5 (1)
O(1)–Cu–N(3)	88.2 (1)	N(2)–Cu–N(3)	94.3 (1)
O(1)–C(1)	1.276 (5)	C(7)–N(2)	1.475 (4)
C(1)–C(2)	1.366 (5)	N(3)–C(8)	1.319 (5)
C(1)–C(4)	1.514 (7)	C(8)–N(4)	1.326 (5)
C(2)–C(3)	1.424 (6)	N(4)–C(9)	1.364 (6)
C(3)–C(5)	1.504 (5)	C(9)–C(10)	1.350 (5)
C(3)–N(1)	1.306 (5)	C(10)–N(3)	1.376 (6)
N(1)–C(6)	1.469 (5)	C(9)–C(11)	1.483 (6)
C(6)–C(7)	1.509 (6)		
Cu–O(1)–C(1)	126.7 (3)	C(6)–C(7)–N(2)	109.8 (3)
O(1)–C(1)–C(2)	125.8 (4)	Cu–N(2)–C(7)	107.6 (3)
O(1)–C(1)–C(4)	114.4 (3)	Cu–N(3)–C(8)	124.0 (3)
C(2)–C(1)–C(4)	119.7 (4)	Cu–N(3)–C(10)	131.0 (3)
C(1)–C(2)–C(3)	125.3 (4)	C(8)–N(3)–C(10)	104.8 (3)
C(2)–C(3)–N(1)	122.3 (3)	N(3)–C(8)–N(4)	110.6 (4)
C(2)–C(3)–C(5)	116.3 (4)	C(8)–N(4)–C(9)	109.6 (3)
N(1)–C(3)–C(5)	121.4 (4)	N(4)–C(9)–C(10)	104.0 (4)
Cu–N(1)–C(3)	126.7 (3)	N(4)–C(9)–C(11)	123.2 (4)
Cu–N(1)–C(6)	113.8 (2)	C(10)–C(9)–C(11)	132.7 (5)
C(3)–N(1)–C(6)	119.4 (3)	C(9)–C(10)–N(3)	111.0 (4)
N(1)–C(6)–C(7)	108.6 (3)		

detected by ^{1}H NMR analysis, but, in spite of many attempts, we did not succeed in isolating a pure sample. This is likely due to too low a concentration of I_a-4Me in the reaction mixture since crystals of the predominant isomer I_a-Me are easily obtained by fractional crystallization.

Description of the Structures of [(AE)Cu(5Me-ImH)]ClO_4 (I_b-5Me) and {[(AE)Ni]$_2$(5(4)Me-Im)}ClO_4 (II_a-4(5)Me). The two structures consist of complex mono- or dinuclear cations and perchlorate anions, but they do not include any solvent molecule. They are represented in Figures 2 and 3, while the relevant distances and angles are listed in Table IV and V.

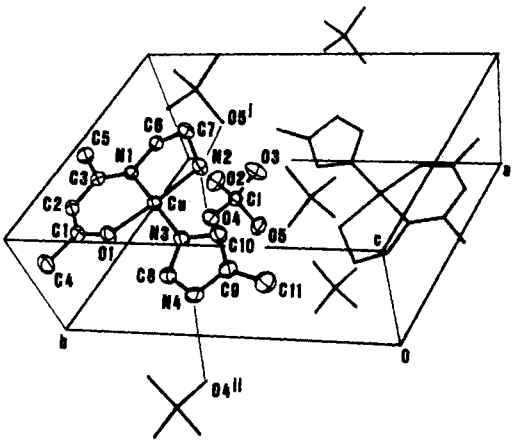

Figure 2. ORTEP plot of [(AE)Cu(5Me-ImH)]ClO_4 (I_b-5Me) with the labeling scheme. Thermal ellipsoids are drawn at 35% probability. Hydrogen atoms are omitted for clarity. Molecular packing is shown with a schematic representation of hydrogen bonds. Symmetry operations are as follows: (i) $x, y, 1 + z$; (ii) $-x, 1 - y, 1 - z$.

Table V. Selected Bond Lengths (Å) and Angles (deg) with Estimated Standard Deviations in Parentheses for II_a-4(5)Me

Ni(1)–O(1)	1.836 (3)	Ni(2)–O(2)	1.840 (3)
Ni(1)–N(1)	1.859 (4)	Ni(2)–N(5)	1.857 (4)
Ni(1)–N(2)	1.912 (4)	Ni(2)–N(6)	1.906 (5)
Ni(1)–N(3)	1.908 (4)	Ni(2)–N(4)	1.897 (4)
O(1)–Ni(1)–N(1)	94.7 (1)	O(2)–Ni(2)–N(5)	96.5 (2)
O(1)–Ni(1)–N(2)	179.0 (1)	O(2)–Ni(2)–N(6)	177.0 (2)
O(1)–Ni(1)–N(3)	87.0 (1)	O(2)–Ni(2)–N(4)	88.8 (1)
N(1)–Ni(1)–N(2)	86.1 (2)	N(5)–Ni(2)–N(6)	85.5 (2)
N(1)–Ni(1)–N(3)	176.2 (2)	N(5)–Ni(2)–N(4)	174.7 (2)
N(2)–Ni(1)–N(3)	92.1 (2)	N(6)–Ni(2)–N(4)	89.2 (2)
O(1)–C(1)	1.297 (5)	O(2)–C(12)	1.294 (6)
O(1)–C(2)	1.356 (7)	C(12)–C(13)	1.378 (8)
C(1)–C(4)	1.500 (7)	C(12)–C(15)	1.478 (8)
C(2)–C(3)	1.395 (7)	C(13)–C(14)	1.365 (9)
C(3)–N(1)	1.318 (6)	C(14)–N(5)	1.326 (7)
C(3)–C(5)	1.506 (7)	C(14)–C(16)	1.510 (8)
N(1)–C(6)	1.456 (6)	N(5)–C(17)	1.450 (9)
C(6)–C(7)	1.490 (7)	C(17)–C(18)	1.481 (9)
C(7)–N(2)	1.470 (6)	C(18)–N(6)	1.456 (8)
N(1)–O(1)–C(1)	125.6 (3)	Ni(2)–O(2)–C(12)	125.5 (3)
O(1)–C(1)–C(2)	124.7 (4)	O(2)–C(12)–C(13)	123.3 (5)
O(1)–C(1)–C(4)	113.5 (4)	O(2)–C(12)–C(15)	115.0 (5)
C(2)–C(1)–C(4)	121.8 (4)	C(13)–C(12)–C(15)	121.6 (5)
C(1)–C(2)–C(3)	125.3 (4)	C(12)–C(13)–C(14)	127.0 (5)
C(2)–C(3)–N(1)	122.0 (4)	C(13)–C(14)–N(5)	122.9 (5)
C(2)–C(3)–C(5)	117.1 (4)	C(13)–C(14)–C(16)	117.8 (5)
N(1)–C(3)–C(5)	121.0 (4)	N(5)–C(14)–C(16)	119.4 (6)
Ni(1)–N(1)–C(3)	126.3 (3)	Ni(2)–N(5)–C(14)	124.4 (4)
Ni(1)–N(1)–C(6)	112.2 (3)	Ni(2)–N(5)–C(17)	113.8 (3)
C(3)–N(1)–C(6)	121.4 (4)	C(4)–Ni(2)–C(17)	121.7 (5)
N(1)–C(6)–C(7)	106.4 (4)	N(5)–C(17)–C(18)	107.8 (5)
C(6)–C(7)–N(2)	106.1 (4)	C(17)–C(18)–N(6)	107.5 (6)
Ni(1)–N(2)–C(7)	108.6 (3)	Ni(2)–N(6)–C(18)	110.1 (4)
N(3)–C(8)	1.338 (6)	C(9)–C(10)	1.359 (6)
C(8)–N(4)	1.328 (6)	C(9)–C(11)	1.461 (8)
N(4)–C(9)	1.379 (6)	C(10)–N(3)	1.364 (6)
Ni(1)–N(3)–C(8)	129.7 (3)	Ni(2)–N(4)–C(9)	126.9 (3)
Ni(1)–N(3)–C(10)	125.5 (3)	N(4)–C(9)–C(10)	107.3 (4)
C(8)–N(3)–C(10)	104.8 (4)	N(4)–C(9)–C(11)	123.0 (4)
N(3)–C(8)–N(4)	112.9 (4)	C(10)–C(9)–C(11)	129.7 (4)
C(8)–N(4)–C(9)	105.6 (4)	C(9)–C(10)–N(3)	109.4 (4)
Ni(2)–N(4)–C(8)	127.4 (3)		

Considering the two figures points to two important observations: (i) the favored mononuclear isomer is the remote one, and (ii) in the dinuclear complex the plane of the adjacent (AE)Ni entity is rotated with respect to the mean plane of the rest of the molecule.

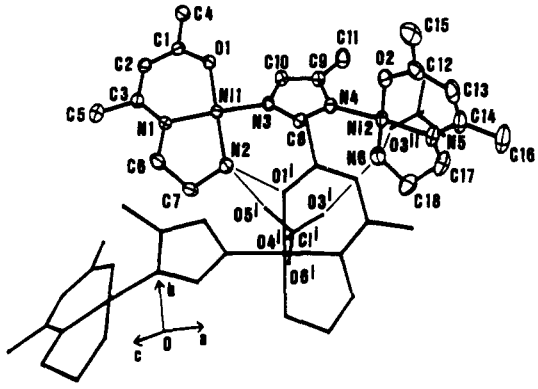

Figure 3. ORTEP plot of [(AE)Ni(4(5)Me-Im)Ni(AE)]ClO_4 (II_a-4(5)-Me) with the labeling scheme. Thermal ellipsoids are drawn at 30% probability. Hydrogen atoms are omitted for clarity. A representation of hydrogen bonds is shown with symmetry operations as follows: (i) $^1/_2 - x, -^1/_2 + y, ^1/_2 - z$; (ii) $^1/_2 + x, ^3/_2 - y, -^1/_2 + z$.

In both complexes, each metal center displays a square-planar coordination involving two nitrogen and one oxygen atoms from the AE ligand and a nitrogen atom from the imidazole (or imidazolate). Least-squares-planes fits show tetrahedral distortions; the deviations from an idealized square-planar geometry are larger (~0.07 ± 0.01 Å) for the mononuclear complex than for the dinuclear one (~0.03 ± 0.01 Å). The imidazole ring is planar in both complexes, the largest deviation from the mean plane being 0.006 (5) Å.

The dihedral angle between the mean planes through AE and 5Me-ImH, respectively, is equal to 13.1 (2)° in complex I_b-5Me. A rather similar geometry is observed for one moiety of the molecule II_a-5Me with a dihedral angle of 22.4 (3)° between the planes through $[(AE)Ni]_R$ and the imidazole ring, respectively, while the plane of the adjacent entity $[(AE)Ni]_A$ is almost orthogonal [92.8 (4)°] to the plane of the imidazole. It may be recalled that, in the heterodinuclear complex [(AE)Ni(Im)Cu(AE)]$^+$ (Im standing for the unsubstituted imidazolate ion), the two (AE)M entities are not far from being coplanar with the Im ring.[1]

This gives an important support to our hypothesis[2] concerning the steric demand of the methyl substituent at position 5 on the imidazolate ring. Steric interactions between this methyl group and the NH_2 or $OCCH_3$ groups of the AE ligand likely prevent the adjacent $[(AE)Ni]_A$ from being approximately coplanar with the rest of the molecule.

The bond lengths between the metal centers and the donor atoms in I_b-5Me and II_a-4(5)Me do not differ significantly from the values reported for similar complexes.[16,26-29] As previously observed,[30] the Ni–ligand bonds are shorter than the homologous Cu–ligand bonds.

The acetylacetone rings are not far from being planar, with no atom deviating from the least-squares plane by more than 0.03 Å. The five-membered rings defined by the metal ions and ethylenediamine are nonplanar and have a gauche conformation in both cases.

Contact distances of less than 3.5 Å are listed in Table VI. For the mononuclear complexes I_b-5Me, the NH_2 group of AE and the pyrrolic NH group of 4(5)Me-ImH are both involved in hydrogen bonding to the O_4 and O_5 oxygen atoms of the perchlorate anion. In the case of II_a-4(5)Me, deprotonation of the pyrrolic NH restricts the possibilities of hydrogen bonding to the

Table VI. Hydrogen Contacts: Bond Lengths (Å) and Angles (deg)[a]

D	H	A	D···A
	(a) I_b-5Me		
N(2)	H(N(2))	O(4)[b]	3.097 (5)
	H_2(N(2))	O(5) (i)[b]	3.108 (5)
N(4)	H(N(4))	O(4) (ii)[b]	2.931 (4)
	(b) II_a-4(5)Me		
N(2)	H(N(2))	O(1) (i)[c]	3.210 (5)
	H_2(N(2))	O(5) (i)[c]	3.218 (12)
N(6)	H(N(2))	O(3) (ii)[c]	2.994 (10)
	H_2(N(6))	O(3) (i)[c]	2.931 (9)

[a] D is the donor atom, A the acceptor one. [b] Symmetry operations (no superscript) x, y, z; (i) $x, y, 1 + z$; (ii) $-x, 1 - y, 1 - z$. [c] Symmetry operations: (i) $^1/_2 - x, -^1/_2 + y, ^1/_2 - z$; (ii) $^1/_2 + x, ^3/_2 - y, -^1/_2 + z$.

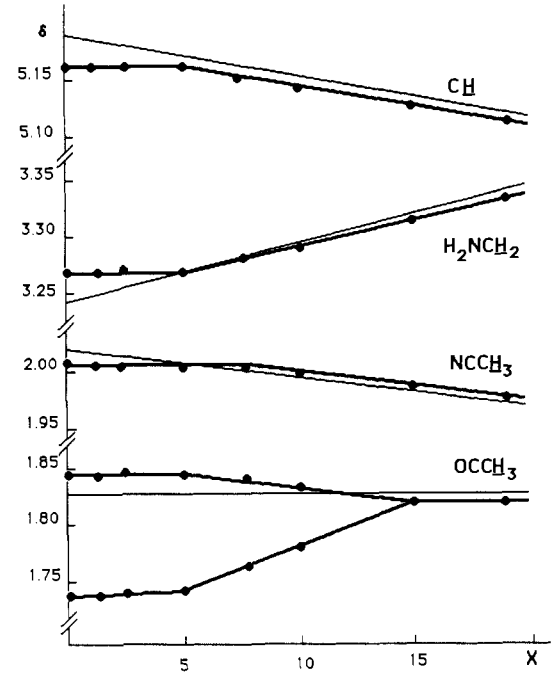

Figure 4. Variations of the shifts δ (ppm) for the AE protons of II_a-4-(5)Me (—) and II_a (—) vs X = [Py]/[Ni] (acetone as solvent, T = 203 K).

NH_2 groups of the AE ligands. One of these NH_2 groups is hydrogen-bonded to two different perchlorate ions, while the second NH_2 is hydrogen-bonded to a perchlorate ion and a ketonic group from a neighboring AE ligand.

^{1}H NMR Spectroscopy. As previously noted, the possibility of steric interactions and subsequent alteration of the coplanar geometry have been first suggested by ^{1}H NMR data.[2]

The data relevant to the present discussion are recalled in Table VII. The adjacent isomer of I_a-4Me has not been isolated, but its NMR characteristics have been determined by comparing the spectrum of a mixture of both isomers and that of the isolated remote isomer.

In contrast with the ^{1}H spectrum of [(AE)Ni(Im)Ni(AE)]$^+$ (II_a), which displays one set of signals for the AE protons, two sets of signals with identical intensities are observed in the case of II_a-4(5)Me. Furthermore, these two sets of signals have δ values almost identical with those observed for the adjacent I_a-4Me and remote I_a-5Me mononuclear isomers, respectively. These data are fully consistent with the structural determination. The inequivalence of the AE moieties as observed in the ^{1}H NMR spectrum of II_a-4(5)Me has to be related to the different orientations of these moieties with respect to the imidazole plane. Furthermore, it may be suggested that, in I_a-5Me, the ligands AE and 5Me-ImH are approximately coplanar as it happens for I_b-5Me.

In the presence of pyridine, I_a-5Me and II_a-4(5)Me become paramagnetic (vide infra) and their ^{1}H NMR spectra are affected

(26) Drew, M. G. B.; McCann, M.; Nelson, S. M. *J. Chem. Soc., Dalton Trans.* **1981**, 1868.
(27) Coughlin, P. K.; Martin, A. E.; Dewan, J. C.; Watanabe, E. I.; Bulkowski, J. E.; Lehn, J. M.; Lippard, S. J. *Inorg. Chem.* **1984**, *23*, 1004.
(28) Matsumoto, N.; Akui, T.; Murakami, H.; Kanesaka, J.; Ohyoshi, A.; Okawa, H. *J. Chem. Soc., Dalton Trans.* **1988**, 1021.
(29) Matsumoto, N.; Yamashita, S.; Ohyoshi, A.; Kohata, S.; Okawa, H. *J. Chem. Soc., Dalton Trans.* **1988**, 1943.
(30) Adams, H.; Bailey, N. A.; Baird, I. S.; Fenton, D. E.; Costes, J.-P.; Cros, G.; Laurent, J.-P. *Inorg. Chim. Acta* **1985**, *101*, 7.

Table VII. ^{1}H NMR Data (δ in ppm versus TMS with CD_3COCD_3 as a Solvent) at 203 K[a]

	$OCCH_3$	$NCCH_3$	NCH_2	H_2NCH_2	CH	$H(2)$	$H(4)$	$H(5)$
$(I_a\text{-}5Me)_R$	1.85	2.11	3.35	2.65	5.25	7.98	6.78	(2.29)[b]
$(Ia\text{-}4Me)_A$	1.74	2.11	3.35	2.65	5.22	8.47	(2.84)[b]	7.18
$(IIa\text{-}4(5)Me)_R$	1.85	2.05	2.58	3.28	5.18	7.35	6.26	(2.58)[b]
$(IIa\text{-}4(5)Me)_A$	1.73	2.05	2.58	3.26	5.15	7.35	(2.58)[b]	6.26

[a] This low temperature is necessary to observe narrow signals. [b] Methylimidazole resonances.

by isotropic shifts, as are their homologues I_a, I_a-1Me, I_a-2Me, and II_a. However, while the behavior of I_a-5Me is identical with that of the other mononuclear complexes,[5] significant differences are observed between II_a-4(5)Me and II_a. In Figure 4, we have represented the dependence of the chemical shifts of the AE protons on the ratio [Py]/[Ni], for these two complexes. The NCH_2 protons are not considered since their signal overlaps with that of the methyl substituent onto the imidazole ring.

Obviously the major difference is for the $OCCH_3$ nuclei. In the case of II_a-4(5)Me, the two signals remain separate until [Py]/[Ni] $\sim$ 15, where they merge into a single signal that has a chemical shift almost identical with that of the same nuclei in II_a, i.e., 1.82 ppm. To reach this position, the two signals have been affected by opposite isotropic shifts. The signal with an initial δ of 1.85 ppm is slightly shielded as is the related absorption in II_a, while the signal with an initial δ of 1.73 ppm suffers a more important deshielding. It may be noted that the slight inequivalences observed for the H_2NCH_2 and CH protons of II_a-4(5)Me vanish as soon as pyridine is added to the solution.

As suggested by a reviewer, an alternative explanation for the similar behaviors of II_a-4(5)Me and II_a in the presence of an excess of pyridine would be that the bridging structures are actually broken. This would result in the formation of mononuclear species such as $[(AE)NiPy_3]^+$, or $[(AE)Ni(ImH)Py_2]^+$ and $[(AE)NiPy_3]^+$. Such a possibility is neither consistent with the electronic spectra results nor with the magnetic data (vide infra).

A more careful examination of Figure 4 points to another difference between the two dinuclear complexes. In the case of II_a, the nuclei begin to move upfield or downfield as soon as pyridine is added, while the nuclei of II_a-4(5)Me remain unaffected as long as [Py]/[Ni] < 5.

The structural data suggest that the steric demand of the 4-(5)-methyl substituent on the imidazole ring prevents coordination of pyridine onto the adjacent nickel ion and possibly onto the remote one. In this instance a modification of the geometry is needed prior to adduct formation. This modification would correspond to the first step in Figure 4, 0 < [Py]/[Ni] < 5, at the end of which the two $OCCH_3$ are equivalent with a δ value of 1.82 ppm, consistent with a nearly coplanar geometry.

Electronic Spectroscopy. As expected, spectra of acetone solutions are almost identical with Nujol mull spectra, whereas, in pyridine, their overall appearance is modified. Indeed, the spectra for the four complexes are solvent-dependent.

In acetone, the mono- and dinuclear nickel complexes give very similar spectra, with absorptions at 448 and 450, respectively. This location is consistent with a square-planar geometry and characteristic of a fairly strong ligand field. Pyridine solution spectra of the mononuclear complex I_a-5Me are devoid of any absorption at ca. 450 nm but display bands of low intensity at 825, 773, and 545 nm that are attributable[31] to a pseudooctahedral form resulting from axial coordination of pyridine molecules into the nickel ions. These absorptions are also clearly present in the spectra of pyridine solutions of II_a-4(5)Me, but the band characteristic of a square-planar form is still present at 434 nm. This behavior offers some similitude to that previously observed for II_a[3] and points to the simultaneous presence of square-planar and pseudooctahedral forms in donor solvents. The occurrence of pentacoordinated species is unlikely since we could not observe bands around 1500 nm.[32]

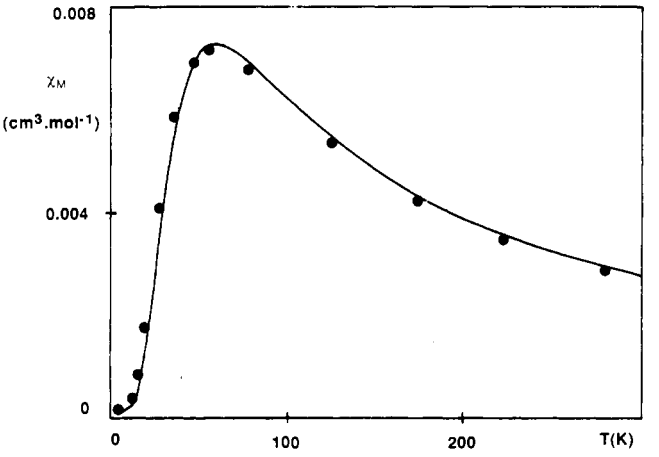

Figure 5. Temperature dependence of the magnetic susceptibility for II_b-4(5)Me.

For the copper complexes, the d–d transitions apparently all occur under a broad envelope that peaks at 560 nm for I_b-5Me and 568 nm for II_b-4(5)Me in acetone solutions and Nujol mull spectra. This position is consistent with a planar or weakly tetrahedral geometry. Replacing the inert solvent by pyridine shifts the maximum to 590 nm for both complexes in accordance with an enlargement of the coordination number of the copper ion from four to five or six.[33]

Magnetic Measurements. The mono- and dinuclear nickel complexes are diamagnetic in the solid state and in solution (acetone). However, when pyridine is added to these solutions, paramagnetism becomes discernible and the calculated values of the effective moment depend on the amount of pyridine. In a large excess of base, [Py]/[Ni] $\geq$ 30, the limiting values of the moment per molecule are equal to 3.0 μ_B (I_a-5Me) and 2.5 μ_B (II_a-4(5)-Me).[19] The former value is within the range of the values expected for high-spin nickel(II) complexes, but the latter one is significantly lower. A priori this discrepancy may be due either to an incomplete conversion of the low-spin forms to the high-spin forms or to the occurrence of antiferromagnetic interactions between the high-spin nickel(II) ions. The ligand field spectrum, which displays absorption attributable to square-planar and pseudooctahedral geometries, supports the first explanation. Furthermore, examples of incomplete conversion have been previously reported. In the presence of an excess of pyridine, the complexes II_a[3] and $[Ni(AE\text{-}Im)Ni(AE)]^{+4}$ (AE-Im stands for a ligand in which the imidazole moiety is linked to the AE moiety through the amino nitrogen atom) (cf. Figure 1) display a moment of 3.0 μ_B in accordance with only one high-spin nickel per binuclear unit. In the present case, there would be statistically less than one high-spin nickel per binuclear unit. Finally it may be noted that these reduced moment values afford a direct proof for the preservation of dinuclear entities in neat pyridine. Indeed, breaking of the bridging structure in II_a-4(5)Me would result in the formation of two mononuclear high-spin complexes with an overall magnetic moment of ca. $3\sqrt{2} = 4.2$ μ_B.

As for the copper complexes, susceptibility measurements have been performed on solid samples from 290 to 5 K. Obviously the mononuclear complex I_b-5Me is paramagnetic. The data corrected for diamagnetism are well fitted to a Curie law, $\chi_A = C/T$ with $C = 0.385$ K cm^3 mol^{-1}. This C value corresponds to $g = 2.10$,

(31) Holm, R. H. *J. Am. Chem. Soc.* **1961**, *83*, 4683.
(32) Dakternieks, D. R.; Graddon, D. P.; Lindoy, L. F.; Mockler, G. M. *Inorg. Chim. Acta* **1973**, *7*, 467.
(33) Hathaway, B. J. *Struct. Bonding (Berlin)* **1954**, *57*, 55.

Table VIII. Structural Parameters (Angles) and Singlet–Triplet Separation for Selected Dicopper Imidazole-Bridged Complexes[a]

	α[b]	θ[c]	$-2J$[d]	ref
$[Cu_2(TMDT)_2(Im)(ClO_4)_2]^+$	160.2	90.0	51.6	15
	161.9	91.8		
$[Cu_2L(Im)]^{3+}$	158.9	68.8	42.0	26
	166.3	79.1		
$[Cu_2(Gly\text{-}GlyO)_2(Im)]^-$	157.5	5.8	38.0	16
	157.2	10.4		
II_b	(162.3)	(11.8)	43.0	1
II_b-4(5)Me	(163.0)	(22.4)	68.0	*e*
	(161.0)	(92.8)		

[a] Ligand abbreviations: Im, imidazole; TMDT, 1,1,7,7-tetramethyldiethylenetriamine; L, 30-membered macrocycle prepared from 2,6-diacetylpyridine and 3,6-dioxooctane-1,8-diamine; Gly-GlyO, glycylglycinate(2–). [b] Angle (deg) between Cu–N and N–N(Im) vectors. [c] Angle (deg) between the copper coordination plane and the imidazole plane. [d] Singlet–triplet separation (cm^{-1}). [e] This work, see text.

typical of a copper(II) ion. The data obtained for the dicopper complex II_b-4(5)Me are represented in Figure 5 in the form of the temperature dependence of χ_M (corrected for diamagnetic contributions and temperature-independent paramagnetism), which points to an antiferromagnetic behavior. The absence of a Curie tail at low temperatures indicates that the sample is free of paramagnetic (mononuclear) impurity so that the data may be fitted to the Bleaney–Bower expression for isotropic exchange in copper(II) dinuclear species.[34] A good agreement between calculated and experimental values is obtained with $g = 2.10$ and $2J = -68\ cm^{-1}$ ($R = 1 \times 10^{-3}$, with $R = \sum(\chi_{obs} - \chi_{calc})^2/\sum(\chi_{obs})^2$).

The susceptibility of I_b-5Me and II_b-4(5)Me has also been determined in solution (acetone) at room temperature.[19] The resulting values of the effective moment are almost identical with those obtained for solid samples, i.e., 1.8 μ_B (I_b-5Me) and 2.5 μ_B (II_b-4(5)Me).

The occurrence of an antiferromagnetic interaction in II_b-4-(5)Me is not unexpected, but the magnitude of the singlet–triplet separation ($2J$) deserves comment. Indeed, this value is significantly greater than those obtained for closely related complexes:

$$2J = -43\ cm^{-1}\ (II_b)^1$$
$$= -44\ cm^{-1}\ (II_b\text{-}2Me)^{35}$$
$$= -40\ cm^{-1}\ (II_b\text{-}Bz)^{35}$$
$$= -48\ cm^{-1}\ (Cu(AE\text{-}Im)Cu(AE))^{+4}$$

(Bz stands for bridging benzimidazolate and AE-Im for the ligand designed earlier).

Several studies have already been reported in which structural data have been used to find correlations between structure and magnetic coupling in imidazolate-bridged dicopper(II) complexes.[15,36,37] The proper conclusion, supported by a theoretical study,[38] is that the magnitude and sign of the coupling constant depend primarily on the angles α between Cu–N(Im) and N–N(Im) vectors, but that they are also affected by the dihedral angles θ between the copper coordination planes and the imidazole plane.

The structural parameters of II_b-4(5)Me have not been determined due to the lack of suitable crystals, but it is not unrealistic to assume that the structure of this complex does not appreciably differ from that of II_a-4(5)Me. In this structure, examination of Table VIII shows that the high value of $2J$ that characterizes II_b-4(5)Me is hardly attributable to α but may originate in the fact that one (AE)Cu moiety is nearly orthogonal to the mean plane defined by the second (AE)Cu entity and the imidazole ring. This would be qualitatively consistent with the conclusion of the theoretical analysis performed[38] on model complexes $[(CuCl_3)_2Im]$ and $[(Cu(NH_2)_3)_2Im]$: for small values of α (i.e., $\alpha < 158°$) the extent of antiferromagnetic coupling increases on increasing θ from 0 to 90°. It may be recalled that this effect is related to the overlap of the imidazolate orbitals and those of a second ligand (AE in the present case) in the coordination sphere of the metal.

Finally, this work emphasizes the importance of steric effects resulting from the presence of a methyl group at position 4 onto the imidazole ring. To relieve these constraints, the mononuclear complexes adopt an isomeric form that places the methyl substituent far from the donor nitrogen atom, while, in the dinuclear complexes, the coordination plane of the adjacent (AE)M unit is rotated so as to become orthogonal to the mean plane of the rest of the molecule. However there is a recent example of "adjacent coordination" for a mononuclear copper complex, but, in this case, the structure was imposed by chelation.[8] The orthogonality of the coordination planes is responsible for the relatively high $2J$ value observed for the dicopper complex. As for the dinickel complex, the relative orientations of the two (AE)Ni units around 4-(5)MeIm likely hinder axial coordination of ligands (pyridine) so that the overall geometry of the molecule has to be modified prior to adduct formation. NMR data are consistent with such a reorientation. Furthermore, it may be noted that, even in pure pyridine, the dinickel complex does not become fully paramagnetic. This may result from the simultaneous presence of pseudooctahedral paramagnetic forms and square-planar diamagnetic forms.

Acknowledgment. We thank Dr. Mari for his contribution to the magnetic measurements.

Supplementary Material Available: Tables SI–SIV for I_b-5Me and Tables SV–SVIII for II_a-4(5)Me, listing fractional atomic parameters, anisotropic thermal parameters, bond lengths and angles, and least-squares-plane equations (13 pages); tables of calculated and observed structure factor amplitudes (28 pages). Ordering information is given on any current masthead page.

(34) Bleaney, B.; Bowers, K. D. *Proc. R. Soc. London, Ser. A* **1952**, *214*, 451.
(35) Costes, J.-P.; Laurent, J.-P. Unpublished data.
(36) Haddad, M. S.; Hendrickson, D. N. *Inorg. Chem.* **1978**, *17*, 2622.
(37) Dewan, J. C.; Lippard, S. J. *Inorg. Chem.* **1980**, *19*, 2079.
(38) Bencini, A.; Benelli, C.; Gatteschi, C.; Zanchini, D. *Inorg. Chem.* **1986**, *25*, 398.